Supplementary Materials for

Human Emissions Drive Recent Trends in North Pacific Climate Variations

Jeremy M. Klavans, Pedro N. DiNezio, Amy C. Clement, Clara Deser, Timothy M. Shanahan, Mark A. Cane
Corresponding author: jeremy.klavans@colorado.edu

The PDF file includes:

Figs. S1 to S11

Tables S1 to S7

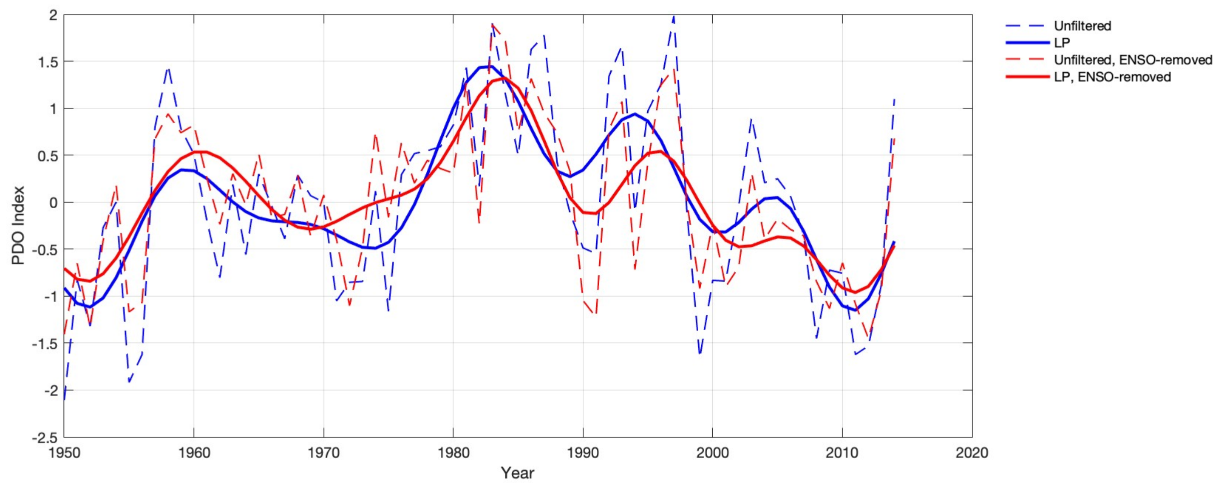

Figure S1. Effect of ENSO removal on the observed PDO index. Observed PDO index timeseries (from NOAA) with and without linearly-removing ENSO for unfiltered (annual average) and low-pass (LP) filtered data.

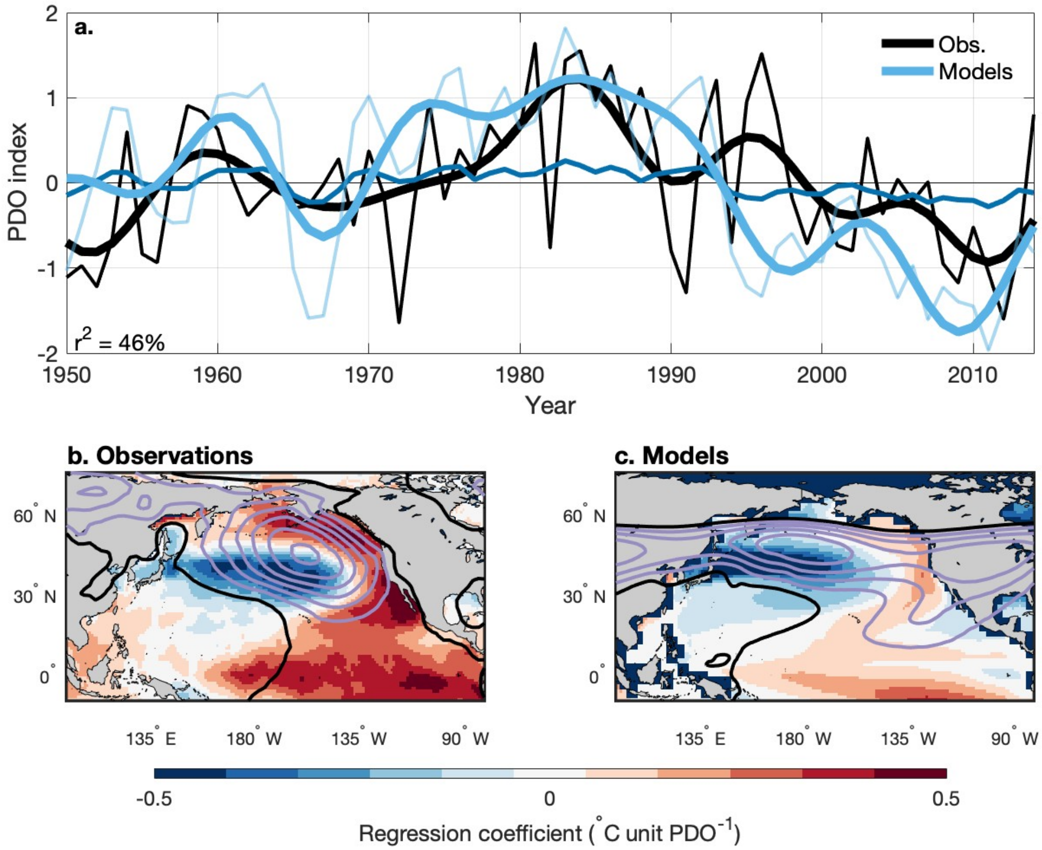

Figure S2. Sensitivity of the role of forcing to the definition of the PDO index. The PDO index in all panels is defined as the 1st principal component of North Pacific sea-surface temperatures after removing North Pacific average SSTs (Methods). (a) The observed PDO index (black) compared with the ensemble mean PDO index from the all-forcings simulations (dark blue) and the normalized ensemble mean PDO index from the all-forcings simulations (light blue). We normalize the forced PDO index strictly to illustrate the timing of the shifts in both indices; the amplitudes of each timeseries are listed in Table S3 and discussed in-text. (b) Regression of observed SST (colors) and sea-level pressure (contours; hPa per unit of the PDO index) on the observed PDO index. We draw contours every -0.5 hPa in purple; the zero contour is in black. The KOE region is outlined in solid black. (c) Regression of forced SST (colors) and sea-level pressure (contours) on the normalized, forced PDO index.

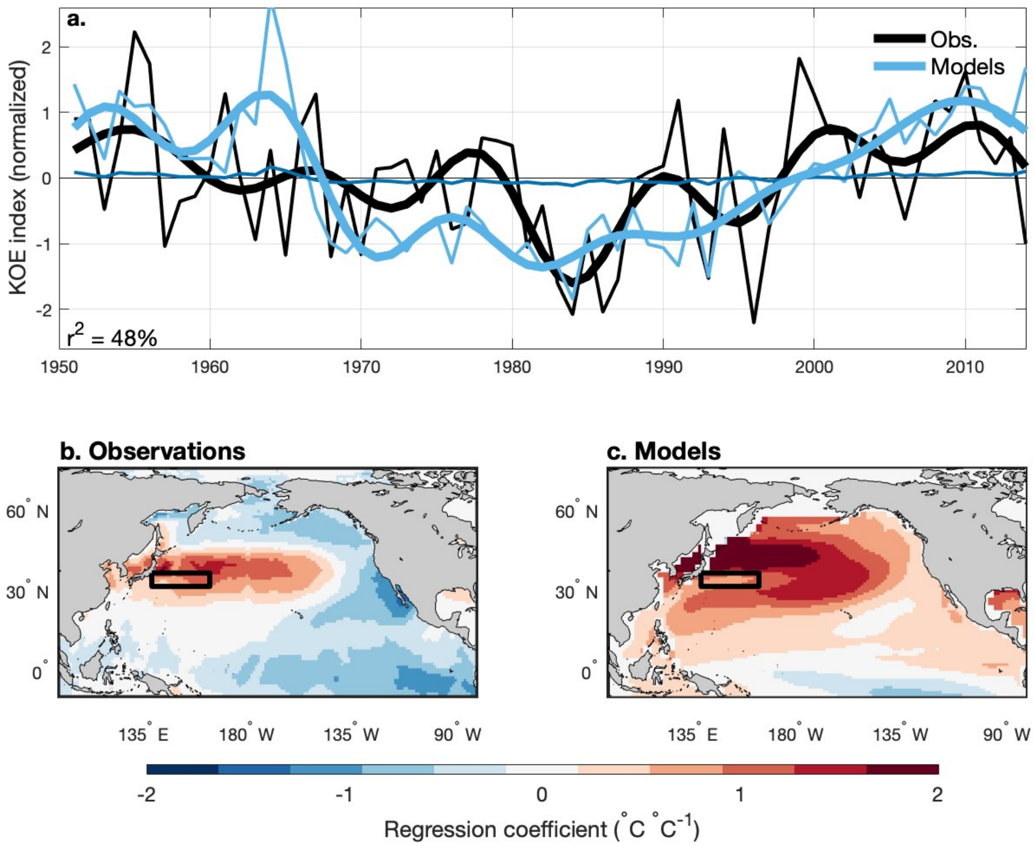

Figure S3. The role of external forcing in a sea-surface temperature index. An index of linearly detrended, spatial-average sea-surface temperatures in the Kuroshio-Oyashio Extension region of the North Pacific is calculated (31° – 36°N, 140° – 165°E; black outline) and regressed on SSTs in observations and models, which shows that the forced signal described in-text is not an artifact of the method we use to calculate the PDO index. a) The detrended, observed KOE sea-surface temperature index (black) compared and the detrended ensemble mean KOE SST index (dark blue) and the normalized, detrended, ensemble mean KOE SST index from the all-forcings simulations (light blue). We normalize the forced KOE index strictly to illustrate the timing of the shifts in both indices; the amplitudes of each timeseries are listed in Table S3 and discussed in-text. (b) Regression of observed SST (colors) on the observed, detrended, KOE index. (c) Regression of forced SST (colors) on the normalized, detrended, forced KOE index.

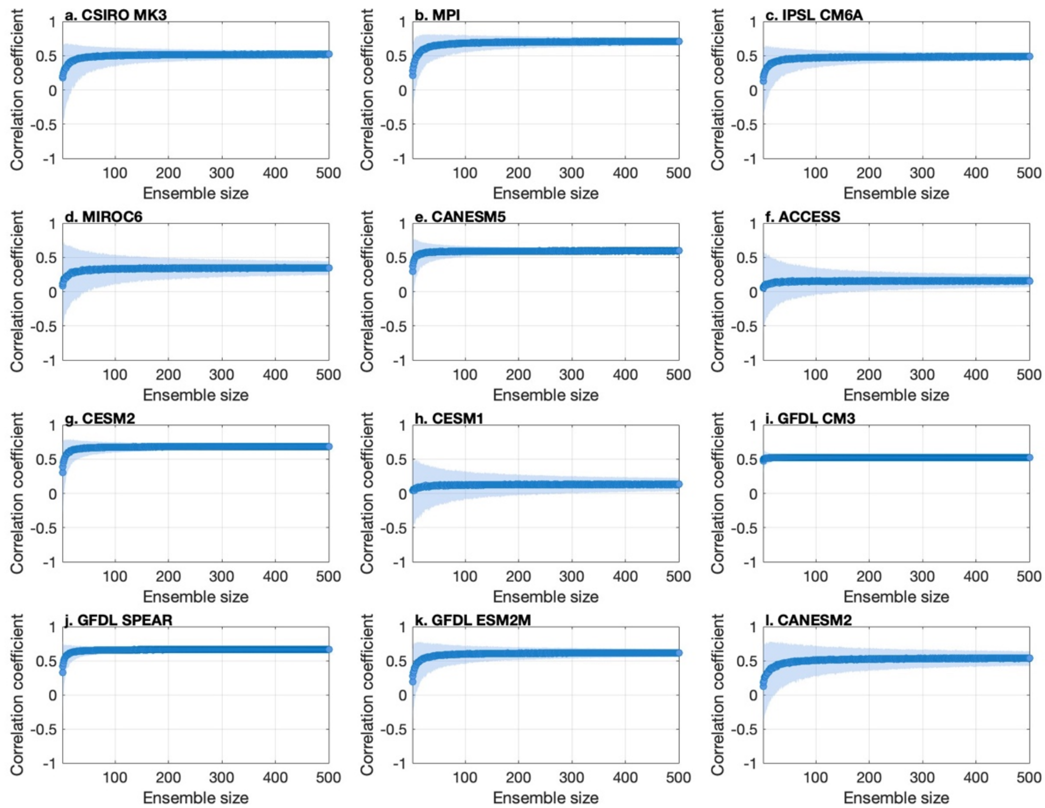

Figure S4. Correlation between the ensemble mean and observed PDO index as a function of ensemble size. As in Fig. 2a, for each ensemble size, we randomly select members from the full ensemble, average, and correlate with observations to calculate the mean explained variance (dot) and the 95% confidence interval (cloud). Please note that this figure reports the correlation coefficient not its square, explained variance, because some values are negative. Additionally, re-sampling with replacement may give a false sense of stability and significance for the correlations calculated from smaller ensembles.

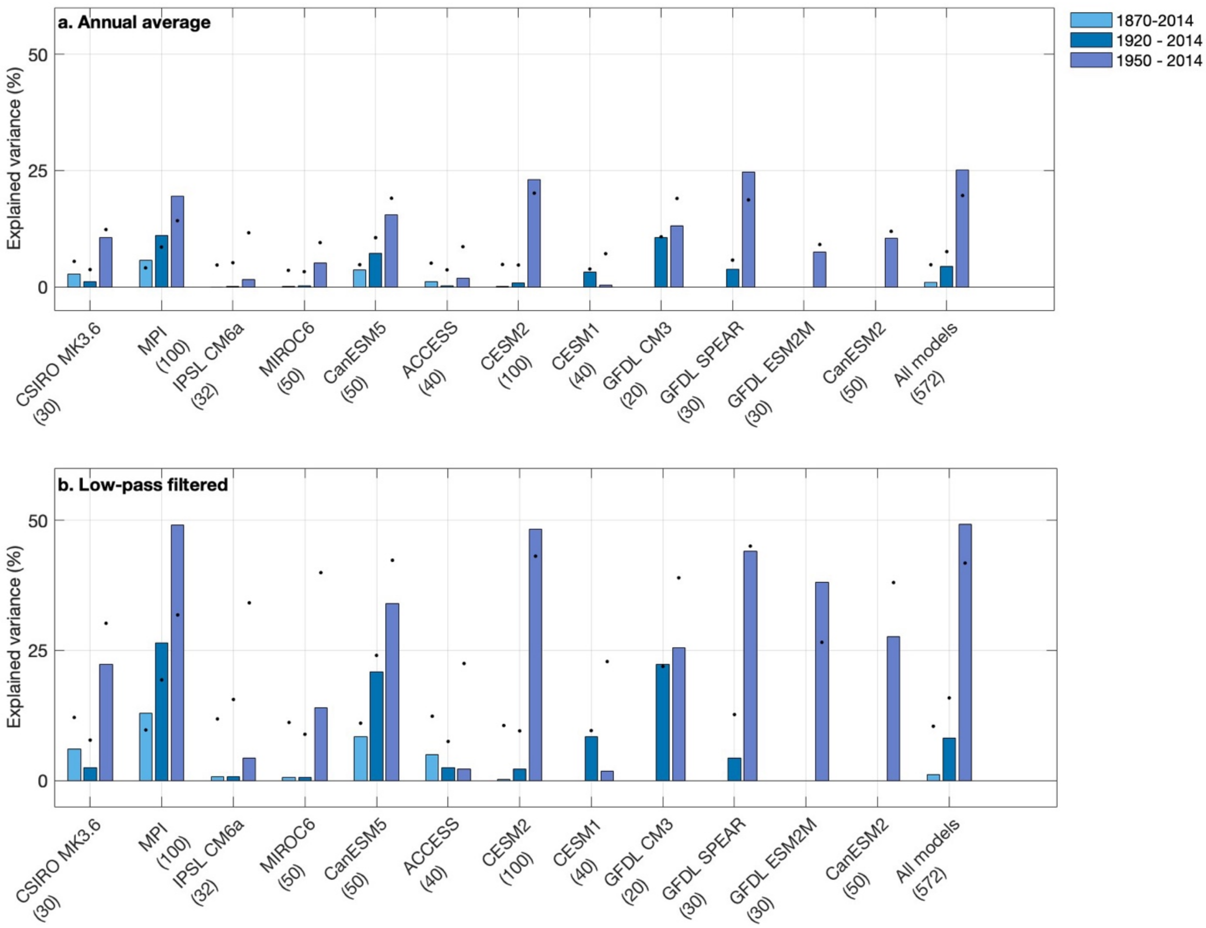

Fig. S5. The evolving role of external forcing in the PDO. External forcing explains more PDO variance after 1950 on both (a) interannual and (b) multidecadal timescales. Please note we only plot bars where model output allows; not all models were initialized prior to 1870 (see Table S1). Also, the number of simulations in each single-model ensemble varies (listed below model name and in Table S1) implying that these bars may not be directly comparable to each other, especially for those models with fewer simulations. Also, the "all models" value varies slightly from the text because we calculate the first principal component of North Pacific SST earlier than 1950 in those models that allow. The black dots correspond to the empirical 90% confidence level, as calculated via phase re-shuffling.

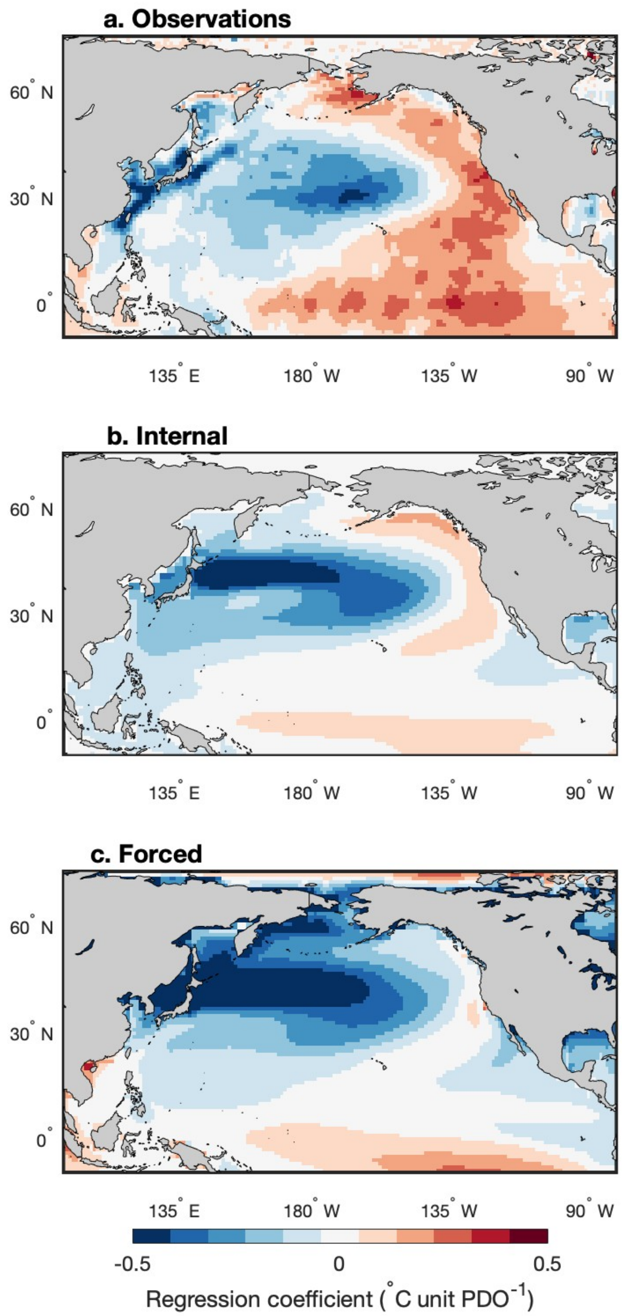

Figure S6. **The PDO pattern from observations, models, and the model ensemble mean.** Panels (a) and (c) correspond to Fig. 1b and 1c in the main text. Panel (b) is taken by averaging the PDO spatial pattern from each individual model run in the ensemble and averaging these patterns.

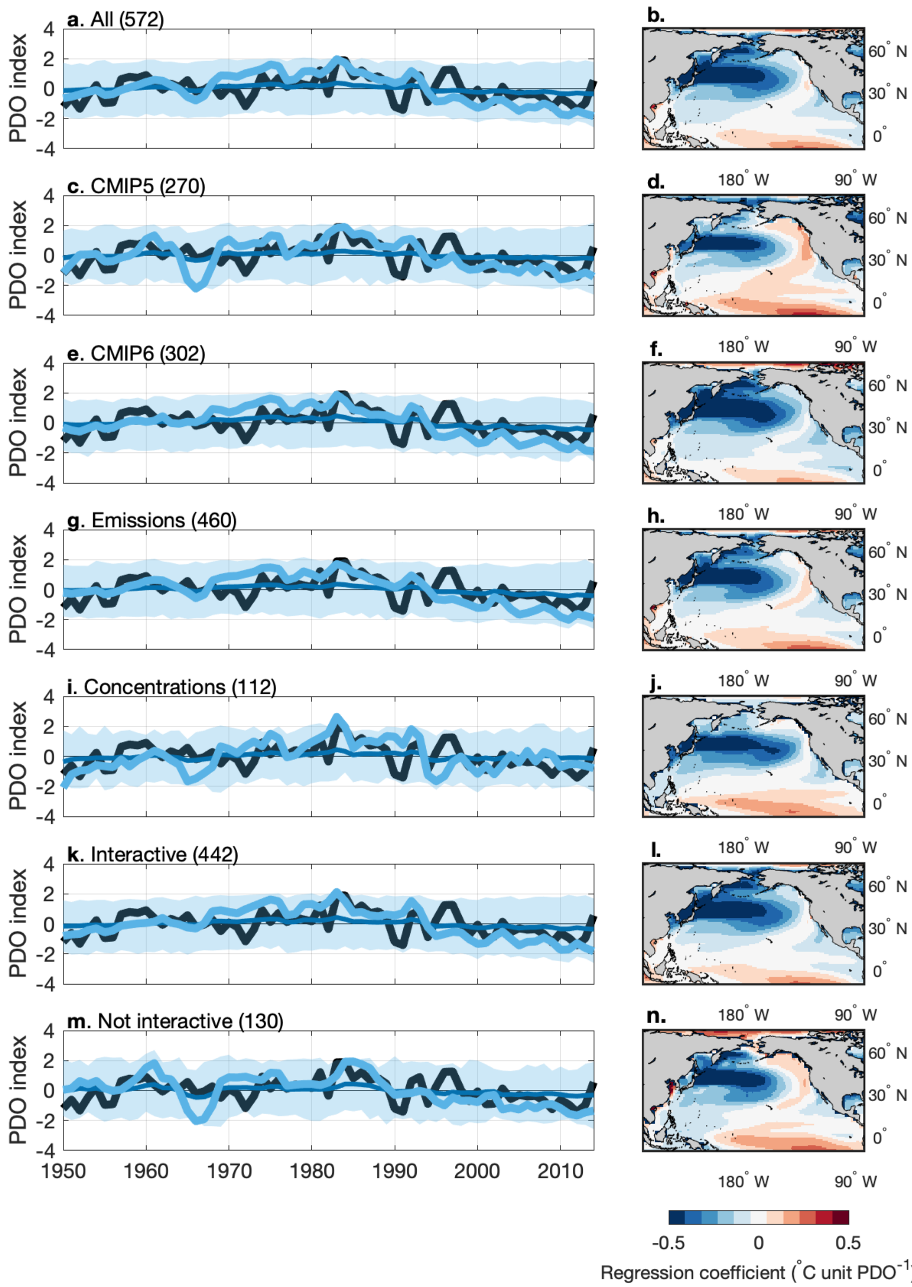

Figure S7. Testing the sensitivity of the explanatory power of the forced PDO to different model configurations (defined in Table S1). (Left panels) The observed PDO index (black) compared with the ensemble mean PDO index from the all-forcings simulations (dark blue) and the normalized ensemble mean PDO index from the all-forcings simulations (light blue). (Right panels) Regression of ensemble mean SST (colors) on the normalized, ensemble mean PDO index. The number of members in each ensemble is listed in parentheses next to the description.

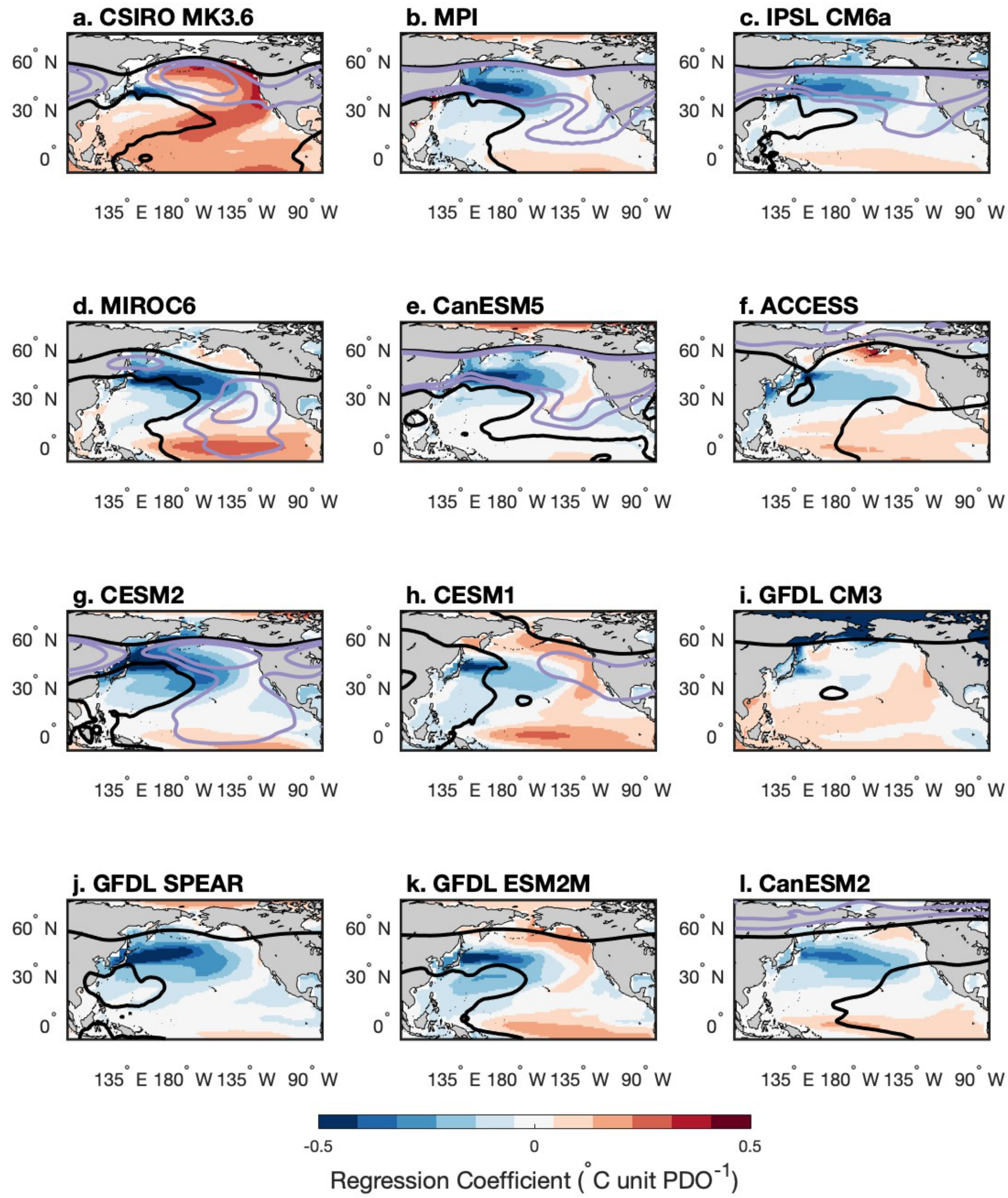

Figure S8. The forced PDO pattern in each large single-model large ensemble. As in Fig. 1c. but for the single model large ensembles listed in Table S1.

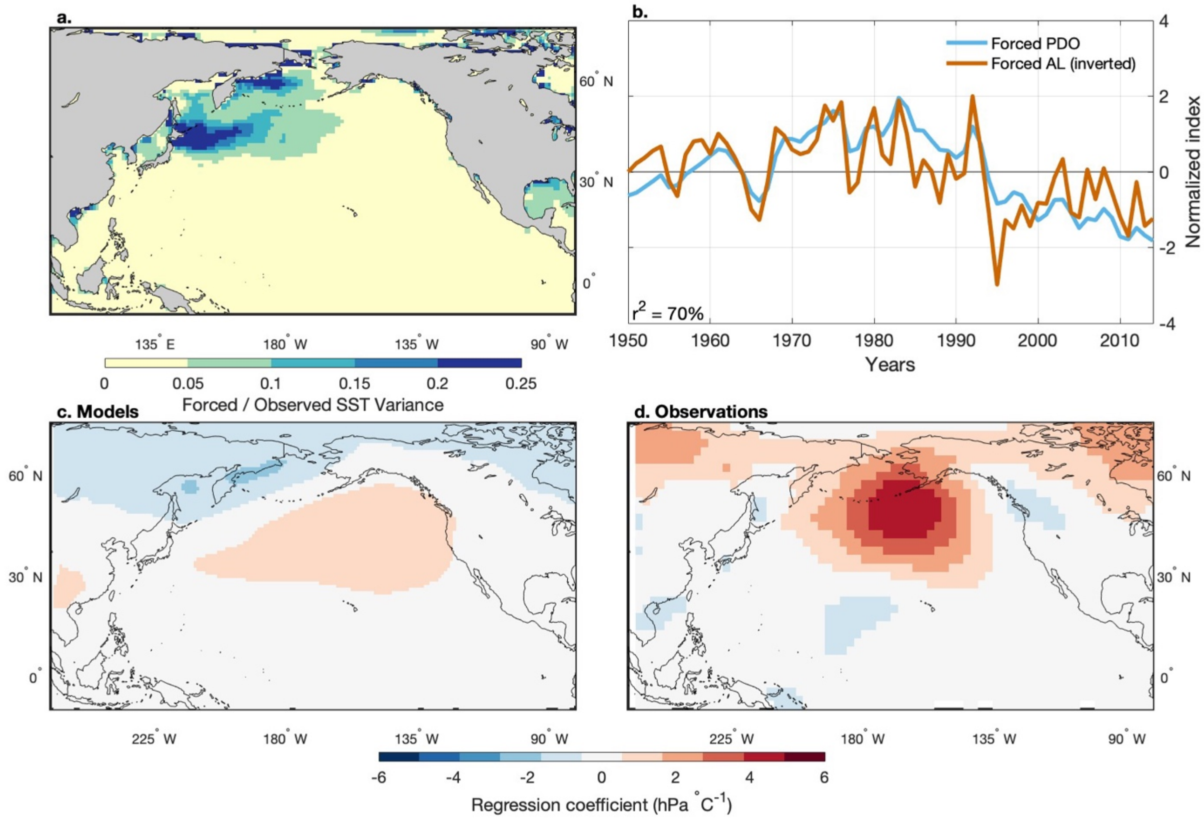

Figure S9. The signal-to-noise paradox in the PDO is associated with weak Aleutian Low variability. (a) The ratio of forced SST variance from models to total observed SST variance in models. (b) Timeseries of the forced PDO (from Fig. 1a) along with the strength of the forced Aleutian Low (as described by the North Pacific Index; Methods) (c) The regression of forced sea-level pressure on an index of forced SST in the KOE region (outlined in Fig. 1b) which indicates the strength of the association between the forced atmospheric response and the forced sea-surface temperature changes. (d) The regression of observed sea-level pressure on the index of observed SST in the KOE region which indicates the strength of the association between the observed atmospheric response and the observed sea-surface temperature changes.

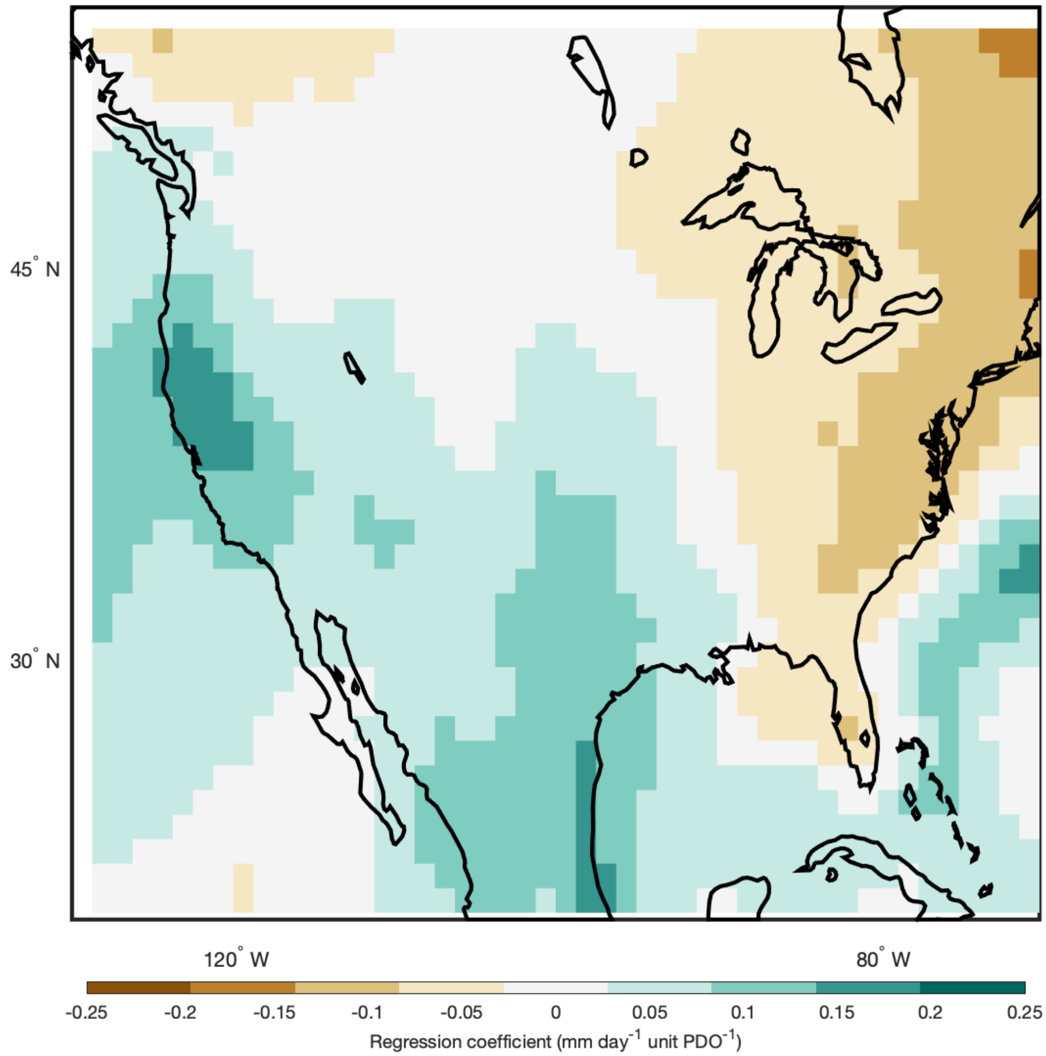

Figure S10. Forced precipitation pattern associated with the forced PDO. Regression of low-pass filtered ensemble mean precipitation anomalies (mm day-1) on the normalized low-pass filtered ensemble mean PDO index.

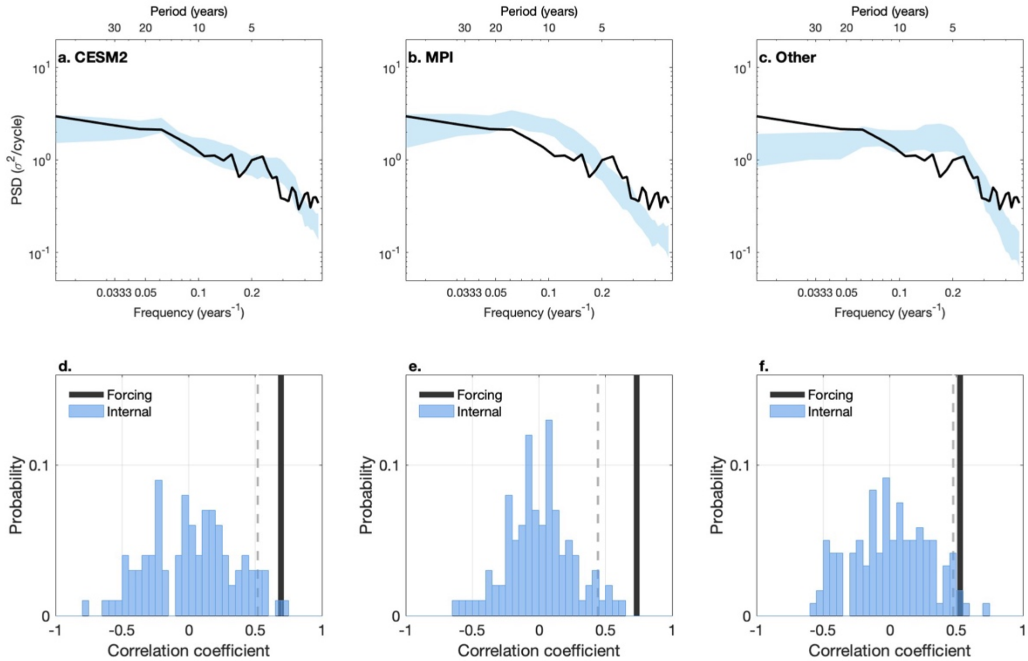

Fig. S11. Role of model PDO realism on signal-to-noise metrics. Here we compare the two single model ensembles with the largest (most realistic) PDO variance (a, b, d, e) with the multimodel ensemble composed of the three single model ensembles with the lowest (least realistic) PDO variances. (a, b, c) The normalized power spectra of the observed PDO (black) and interquartile range of PDO indices produced by individual ensemble members (blue cloud). (d, e, f) Comparison of the correlation coefficient between the internally-generated PDO indices in individual ensemble members and observations (blue histogram) with the correlation coefficient of the ensemble mean and observation (black vertical line). The empirical 90% confidence level (two-tailed) for the distribution of correlations is displayed with a light gray vertical line.

CMIP5 Ensembles	Atmospheric resolution	# of members (270)	Start year	Emissions vs. concentrations	“Fully-interacive” (AR5 Table 9.1)
NCAR-CESM1	1deg	40	1920	Emissions	Yes
GFDL-CM3	2deg	20	1920	Emissions	Yes
GFDL-ESM2M	2deg	30	1950	Concentration	No
CCCma-canESM2	2.8deg	50	1950	Concentration	Yes
CSIRO-Mk3	1.9deg	30	1850	Emissions	Yes
MPI-ESM-LR	1.9deg	100	1850	Emissions	No
CMIP6 Ensembles	Atmospheric resolution	# of members (302)	Start year		
NCAR-CESM2	1deg	100	1850	Emissions	Yes
GFDL-SPEAR	0.5deg	30	1921	Emissions	Yes
IPSL-CM6A-LR	~2deg	32	1850	Concentration	Yes
MIROC6	~2deg	50	1850	Emissions	Yes
canESM5	~2deg	50	1850	Emissions	Yes
ACCESS-ESM1.5	~1.5deg	40	1850	Emissions	Yes

Table S1. Additional details on the climate models studied[62, 69 - 79]. Classifications for cloud-aerosol interactions are constructed to match those in[14].

Model	**Aerosol-only (75)**	**GHG-only (82)**	**Natural-only (129)**
canESM5	30	50	50
CNRM-CM6	10	9	10
GISS-E2_1_G	15	10	20
IPSL CM6A LR	10	10	8
MIROC6	10	3	41

Table S2. The single-forcing ensembles and their respective sizes used in this study (from DAMIP[63].

	Unfiltered Corr. (Sig. Level)	Low-pass Filtered Corr. (Sig. Level)
PDO (GMSST Removed)	0.43 (6%)	0.73 (4%)
PDO (North Pacific Removed)	0.36 (8%)	0.69 (6%)
KOE SST Index	0.34 (9%)	0.68 (4%)

Table S3. Correlation coefficients and their significance levels for the three PDO definitions in the main text. As in the main text, the KOE SST index is detrended. Significance levels are calculated empirically following Ebisuzaki 1997.

Forced Variance	**1870-1949**	**1950-2014**
PDO Index (Unfiltered)	0.02	0.04
PDO Index (LP)	0.02	0.04
KOE SST Index (Unfiltered)	0.01	0.14
KOE SST Index (LP)	0.01	0.13

Table S4. Ensemble mean variance for the PDO index and detrended KOE SST index from the suite of models that were initialized in 1850 (see Table S1). Values are reported for both the annual average indices and the low-pass filtered (LP) indices.

	Forced Variance	**Internal Variance**	**Total variance (Forced plus Internal)**
KOE SST Index (Unfiltered)			
1870 - 1949	0.01	0.36	0.37
1950 - 2014	0.14	0.36	0.50
1870 - 2014	0.08	0.38	0.46
KOE SST Index (LP)			
1870 - 1949	0.01	0.18	0.19
1950 - 2014	0.13	0.18	0.31
1870 - 2014	0.07	0.21	0.28

Table S5. Forced, internal, and total variance in the unfiltered and low-pass filtered (LP) KOE SST index, spliced by time period. The internal variance is calculated by subtracting the ensemble mean KOE SST index from each individual ensemble member's detrended KOE SST index, as in the main text.

Name	**# members**	**R^2 (1950 – 1989)**	**R^2 (1990 – 2014)**	**R^2 (1950 – 2014)**	**S:T PDO**	**S:T KOE SST**	**S:T NPI**
All	572	0.43 (0.01)	0.35 (0.14)	0.53 (0.02)	0.19	0.27	0.09
CMIP5	270	0.51 (0.01)	0.35 (0.14)	0.59 (0.01)	0.15	0.20	0.09
CMIP6	302	0.28 (0.03)	0.36 (0.14)	0.44 (0.05)	0.25	0.34	0.11
Emissions	460	0.37 (0.02)	0.44 (0.12)	0.50 (0.02)	0.21	0.28	0.11
Concentrations	112	0.57 (0.01)	0.03 (0.35)	0.33 (0.07)	0.17	0.23	0.13
Interactive	442	0.35 (0.02)	0.31 (0.15)	0.46 (0.04)	0.20	0.29	0.09
Not interactive	130	0.31 (0.04)	0.58 (0.08)	0.50 (0.01)	0.22	0.27	0.12

Table S6. The timing and amplitude of the forced PDO for ensembles of varying model designs (see Table S1). The R^2 columns report the square of the correlation between the ensemble mean and observed PDO indices for the time period indicated along with its p-value. The p-value is calculated empirically as in Fig. 1a, via phase reshuffling of the ensemble mean in frequency space[31]. For the R^2 columns, significance testing was applied to the correlation. The signal-to-total ratios estimated in the four right-most columns are calculated as the ratio of forced-to-total variance. The "signal-to-noise paradox", described in Methods, emerges when there is a mismatch between the R^2 values and the signal-to-total ratios. Signal-to-total ratios are reported for the PDO index, KOE SST index, and the North Pacific Index (NPI).

Name	**Total number of members**	**R^2 (1950 – 1989)**	**R^2 (1990 – 2014)**	**R^2 (1950 – 2014)**	**S:T PDO (1950-1989)**	**S:T PDO (1990 -2014)**	**S:T PDO (1950 -2014)**
Aerosol-only	75	0.58 (<0.01)	0.16 (0.22)	0.04 (0.40)	0.02	0.01	0.02
GHG-only	82	0.60 (<0.01)	0.57 (0.10)	0.09 (0.31)	0.17	0.19	0.45
Natural only	129	0.38 (0.03)	0.00 (0.52)	0.01 (0.38)	0.02	0.01	0.02

Table S7. Explained variance from single-forcing ensembles described in Table S2 along with their p-values. The p-value is calculated empirically as in Fig. 1a, via phase reshuffling of the ensemble mean in frequency space[31]. For the R^2 columns, significance testing was applied to the correlation. Please note that the correlation coefficient between the GHG-only ensemble mean and observations is negative. The signal-to-total ratios estimated in the three right-most columns are calculated as the ratio of forced-to-total variance.